The Journal of Experimental Biology 211, 2358-2368
Published by The Company of Biologists 2008
doi:10.1242/jeb.015263

Phylogeny, scaling, and the generation of extreme forces in trap-jaw ants

Joseph C. Spagna[1,2,*], Antonis I. Vakis[1,3], Chris A. Schmidt[4], Sheila N. Patek[5], Xudong Zhang[1,3], Neil D. Tsutsui[6] and Andrew V. Suarez[1,2]

[1]Beckman Institute for Advanced Science and Technology, [2]Department of Entomology and Department of Animal Biology, and [3]Department of Mechanical Science and Engineering, University of Illinois at Urbana-Champaign, Urbana, IL 61801, USA, [4]Graduate Interdisciplinary Program in Insect Science, University of Arizona, Tucson, AZ 85721, USA and [5]Department of Integrative Biology, and [6]Department of Environmental Science, Policy and Management, University of California, Berkeley, CA 94720, USA

*Author for correspondence (e-mail: jspagna@uiuc.edu)

Accepted 9 April 2008

SUMMARY

Trap-jaw ants of the genus *Odontomachus* produce remarkably fast predatory strikes. The closing mandibles of *Odontomachus bauri*, for example, can reach speeds of over 60 m s^{-1}. They use these jaw strikes for both prey capture and locomotion – by striking hard surfaces, they can launch themselves into the air. We tested the hypothesis that morphological variation across the genus is correlated with differences in jaw speeds and accelerations. We video-recorded jaw-strikes at 70 000–100 000 frames s^{-1} to measure these parameters and to model force production. Differences in mean speeds ranged from 35.9±7.7 m s^{-1} for *O. chelifer*, to 48.8±8.9 m s^{-1} for *O. clarus desertorum*. Differences in species' accelerations and jaw sizes resulted in maximum strike forces in the largest ants (*O. chelifer*) that were four times those generated by the smallest ants (*O. ruginodis*). To evaluate phylogenetic effects and make statistically valid comparisons, we developed a phylogeny of all sampled *Odontomachus* species and seven outgroup species (19 species total) using four genetic loci. Jaw acceleration and jaw-scaling factors showed significant phylogenetic non-independence, whereas jaw speed and force did not. Independent contrast (IC) values were used to calculate scaling relationships for jaw length, jaw mass and body mass, which did not deviate significantly from isometry. IC regression of angular acceleration and body size show an inverse relationship, but combined with the isometric increase in jaw length and mass results in greater maximum strike forces for the largest *Odontomachus* species. Relatively small differences (3%) between IC and species-mean based models suggest that any deviation from isometry in species' force production may be the result of recent selective evolution, rather than deep phylogenetic signal.

Supplementary material available online at http://www.life.uiuc.edu/suarez/datasets.html

Key words: biomechanics, locomotion, feeding mechanics, *Odontomachus*, evolution.

INTRODUCTION

Arthropods are renowned for their morphological variation, and many species have evolved extreme mechanical abilities for a variety of functions such as the remarkable jumping ability of fleas, and the crushing strikes of stomatopods (Bennet-Clark and Lucey, 1967; Patek et al., 2004). These extreme speeds and accelerations are often achieved with the help of specific innovations such as latches, lever arms, and spring mechanisms that help store and release high amounts of energy (Gronenberg, 1996a). It has been argued that these abilities are optimized in such a way that tradeoffs between mechanical abilities (benefits) and physiological requirements for maintaining them (costs) are balanced against the greatest required performance for that feature (Weibel and Taylor, 1998). But in nature, where animals evolve in response to a variety of selective pressures in a changing environment, optimal performance in any one context may be constrained by physical laws, developmental programs and phylogenetic history. This is particularly true if an adaptive feature or mechanism has multiple functions – optimizing it for one function may result in sub-optimal performance in another, or competing demands may leave performance in an intermediate range for a plurality of functions.

The jaw strikes of trap-jaw ants were characterized morphologically and neurobiologically in a series of papers by Gronenberg and colleagues (Gronenberg, 1995a; Gronenberg, 1995b; Gronenberg, 1996b; Gronenberg and Tautz, 1994; Just and Gronenberg, 1999) and jaw strikes of the species *Odontomachus bauri* Emery 1982 can reach extremely high speeds, of over 60 m s^{-1} (Patek et al., 2006). Beyond providing the ants with the ability to disable prey, the jaw snaps have been evolutionarily co-opted for ballistic locomotion. It has long been known that trap-jaw ants jump (Wheeler, 1922), but only recently has the way they use their jaws to do so been characterized. These movements take the forms of 'bouncer defense' jumps (Carlin and Gladstein, 1989), where the ants are propelled horizontally away from a threat, and 'escape jumps', where the jaws are placed against or aimed at the substrate then fired, launching the ant into the air upon triggering (Patek et al., 2006). However, *O. bauri* is just one of approximately 60 species in the genus *Odontomachus*, and while all members of the genus share the same general trap-jaw morphology, there are morphological and ecological differences between species that provide the basis for comparative study.

Across the pantropically distributed genus *Odontomachus*, species vary considerably in their ecology (Deyrup and Cover, 2004),

Table 1. Primer information

Gene/primer	Sequence (5′ to 3′)	Position	Reference
28S/3318F	CCCCCTGAATTTAAGCATAT	*Drosophila* 3318–3337	(Schmitz and Moritz, 1994)
28S/4068R	TTGGTCCGTGTTTCAAGACGGG	*Drosophila* 4068–4047	(Belshaw and Quicke, 1997)
Wg/Wg550F	ATGCGTCAGGARTGYAARTGYCAYGGYATGTC	*Pheidole* 539–570	(Wild and Maddison, 2008)
Wg/578F	TGCACNGTGAARACYTGCTGGATGCG	*Pheidole* 578–603	(Ward and Downie, 2005)
Wg/BWg WCF	GTRAARACYTGCTGGATGCG	*Pheidole* 584–603	D. R. Maddison (personal comm.)
Wg/1032R	ACYTCGCAGCACCARTGGAA	*Pheidole* 1032–1013	(Abouheif and Wray, 2002)
WG/WgABRz	CACTTNACYTCRCARCACCARTG	*Pheidole* 1038–1016	(Wild and Maddison, 2008)
LWR/LR134F	ACMGTRGTDGACAAAGTKCCACC	*Apis* 134–156	(Ward and Downie, 2005)
LWR/LR639ER	YTTACCGRTTCCATCCRAACA	*Apis* ~639–624	(Ward and Downie, 2005)
COI/Jerry	CAACATTTATTTTGATTTTTTGG	*Apis* 945–967	(Simon et al., 1994)
COI/Pat	ATCCATTACATATAATCTGCCATA	*Apis* 1847–1824	(Simon et al., 1994)

Primer positions are as in GenBank accession numbers M21017 (*Drosophila melanogaster*), AY101369.1 (*Pheidole morrisi*), U26026 (*Apis mellifera*, *LWR*) and M23409 (*Apis mellifera*, *COI*).

including nest site substrates and types of prey, as well as varying morphologically, covering a range of body sizes and mandible lengths. These differences suggest that there may be variation in the performance of the strikes among species (perhaps based on speed or chemical defenses of common prey, or the relative advantage of jumping ability in nests or foraging areas with different physical characteristics) and may provide insight into the co-option of the mandibles for locomotion as well as prey capture. Thus multi-species comparisons are informative for characterizing trap-jaw morphology and performance and, more generally, for understanding how a multi-functional system may be optimized, or constrained, relative to its various functions.

The goals of this study were to: (1) collect kinematic and morphometric data for eight species of the trap-jaw ant genus *Odontomachus*; (2) construct a phylogenetic hypothesis for these species; and (3) generate a model for force production based on phylogenetically corrected body size scaling equations, and compare this modeled range to the observed range across the eight species measured in this study.

MATERIALS AND METHODS

Phylogeny

In order to detect phylogenetic effects in our comparative data, and to correct for the problems of non-independence that can invalidate statistical comparisons between species (Felsenstein, 1985), we developed a phylogenetic hypothesis for a sampling of species, including the eight species for which we collected strike data. We generated sequence data for 19 species including 12 *Odontomachus* and seven outgroup taxa from other ponerine genera. Portions of four genes were used: the mitochondrial gene for cytochrome oxidase 1 (*COI*), the large subunit (*28S*) ribosomal RNA gene, and the nuclear protein-encoding genes *wingless* (*wg*) and *long-wavelength rhodopsin* (*LWR*). Primer information is provided in Table 1. A variable-length intron in the sequenced section of *rhodopsin* proved difficult to align among the outgroup taxa and was included only for the *Anochetus* and *Odontomachus* species. After excluding 29 bp of ambiguously aligned *28S* data we were left with 2685 bp of aligned, concatenated sequence data. Taxon information and GenBank accession numbers are given in Table 2. Final deposition of molecular voucher specimens used in this study (currently held in personal collection of C.A.S.) will be in the United States Museum of Natural History (Smithsonian).

Genomic DNA was extracted from one or two legs of a single adult specimen for each taxon, using the DNEasy Tissue Kit (Qiagen Inc., Valencia, California, USA). PCR amplification generally consisted of 40 cycles of 20 s at 94°C, 20 s at 48°–54°C (typically 48°C for 28S and 50–54°C for the other genes), and 50 s at 65°C, with an initial denaturation of 2 min at 94°C and a final extension

Table 2. Taxon information with GenBank accession numbers for loci sequenced

Taxon	Locality	*28S*	*Wg*	*LWR*	*COI*
Platythyrea strenua	Dominican Republic	EU155423	EU155479	EU155460	EU155441
Hypoponera opacior	USA	EU155410	EU155464	EU155445	EU155427
Plectroctena ugandensis	Gabon	EU155424	EU155480	EU155461	EU155442
Odontoponera transversa	Indonesia	EU155422	EU155478	EU155459	EU155440
Leptogenys attenuata	South Africa	EU155411	EU155465	EU155446	EU155428
Anochetus emarginatus	Trinidad	–	EU155462	EU155443	EU155425
Anochetus princeps	Indonesia	EU155409	EU155463	EU155444	EU155426
Odontomachus bauri	Ecuador	–	EU155466	EU155447	EU155429
Odontomachus brunneus	USA	EU155412	EU155467	EU155448	EU155430
Odontomachus cephalotes	Australia	EU155413	EU155468	EU155449	EU155431
Odontomachus chelifer	Trinidad	–	EU155469	EU155450	EU155432
Odontomachus clarus	USA	EU155414	EU155470	EU155451	EU155433
Odontomachus erythrocephalus	Panama	EU155415	EU155471	EU155452	EU155434
Odontomachus haematodus	Ecuador	EU155416	EU155472	EU155453	EU155435
Odontomachus hastatus	Ecuador	EU155417	EU155473	EU155454	EU155436
Odontomachus opaciventris	Costa Rica	EU155418	EU155474	EU155455	EU155437
Odontomachus relictus	USA	EU155419	EU155475	EU155456	–
Odontomachus ruficeps	Australia	EU155420	EU155476	EU155457	EU155438
Odontomachus ruginodis	USA	EU155421	EU155477	EU155458	EU155439

Table 3. Mean jaw strike, collection, and size data for experimental colonies

Species and authority	Locality	Body mass (mg)	Head width (mm)	Jaw length (mm)	Jaw mass (mg)	Max. strike speed ($m\ s^{-1}$)	Mean max. speed ($m\ s^{-1}$)	Mean max. radial acceleration ($m\ s^{-2}$)	Mean max. single-jaw force (mN)
Odontomachus ruginodis Smith 1937	Florida, USA	5.6 (0.5)	1.62 (0.10)	1.10 (0.03)	0.052 (.007)	50.0	36.5 (7.1)	1.47E+06 (3.96E+05)	25.5 (6.7)
Odontomachus brunneus (Patton 1894)	Florida, USA	7.6 (0.7)	1.79 (0.07)	1.16 (0.01)	0.070 (0.004)	66.5	41.5 (12.1)	1.59E+06 (5.27E+05)	30.2 (11.1)
Odontomachus haematodus (Linnaeus 1758)	P.N. Iguazu, Argentina	6.0 (0.8)	1.60 (0.08)	1.16 (0.07)	0.056 (0.010)	56.8	43.3 (7.2)	1.45E+06 (3.00E+05)	22.0 (7.8)
Odontomachus clarus subs. desertorum Roger 1861	Arizona, USA	10.6 (2.0)	1.98 (0.09)	1.32 (0.09)	0.095 (0.020)	65.3	48.8 (8.9)	1.74E+06 (3.46E+05)	52.9 (12.2)
Odontomachus erythrocephalus Emery 1890	La Selva, Costa Rica	12.7 (0.5)	2.20 (0.07)	1.58 (0.04)	0.144 (0.016)	64.3	46.3 (11.4)	1.57E+06 (5.26E+05)	71.2 (24.4)
Odontomachus cephalotes Smith 1863	Queensland, Australia	16.7 (2.1)	2.28 (0.13)	1.60 (0.05)	0.162 (0.003)	48.3	37.1 (7.7)	1.15E+06 (3.64E+05)	60.5 (22.7)
Odontomachus chelifer Latreille 1802	P.N. Iguazu, Argentina	24.6 (2.8)	2.63 (0.07)	2.15 (0.04)	0.310 (0.032)	53.1	35.9 (7.7)	8.73E+05 (2.18E+05)	85.2 (26.5)
*Odontomachus bauri** Emery 1892	La Selva, Costa Rica	11.6 (2.2)	2.00 (0.08)	1.29 (0.07)	0.131 (.013)	60.0	38.3 (8.7)	1.21E+06 (4.56E+05)	47 (12)

Values are means (± s.d.).
*Data from Patek et al. (Patek et al., 2006).

of 3 min at 65°C. For most amplifications a total reaction volume of 20 μl was used, including 1 unit of HotMaster Taq (Eppendorf AG, Hamburg, Germany), 0.16 mmol l^{-1} dNTP mix (Eppendorf AG, Hamburg Germany), 0.5 μmol l^{-1} each primer, and 1 or 2 μl of DNA template. PCR products were cleaned and sequenced by the GATC core sequencing facility on the University of Arizona campus. Sequences were aligned manually in MacClade 4.08 (Maddison and Maddison, 2005).

Phylogenetic analysis was conducted using a partitioned Bayesian approach in MrBayes 3.1.2 (Huelsenbeck and Ronquist, 2001). Protein-coding genes were partitioned by gene and codon position, with one partition for *28S* and an additional partition for the *rhodopsin* intron (giving 11 total partitions). An exploratory MrBayes analysis was performed in which each partition was given a GTR+I+G model (nst=6, rates=invgamma) and all parameters were unlinked across partitions. Examination of the resulting parameter sampling in Tracer 1.3 (Rambaut and Drummond, 2004) suggested the adequacy of a reduced model: GTR+I (nst=6, rates=propinv) for first and second codon positions and for 28S, HKY+I (nst=2, rates=propinv) for third codon positions of *wingless* and *rhodopsin* and for the *rhodopsin* intron, and HKY+I+G (nst=2, rates=invgamma) for third codon positions of *cytochrome oxidase 1*. A final analysis was performed using this modeling scheme, with variable rates across partitions (prset ratepr=variable) and all other priors left at program defaults.

Two simultaneous independent analyses were run, each with four chains and the default heating value, for a total of five million generations. The consensus tree was generated using the sumt command in MrBayes with a burn-in of one million generations, chosen *post hoc* after examination of parameter convergence in Tracer. Chain mixing was adequate and all parameters (including tree topology) converged rapidly. Equivalent analyses were performed on the mitochondrial and the nuclear data alone to compare results from single genome partitions.

Although the data partitioning and modeling scheme employed in this analysis is probably overparameterized, Bayesian phylogenetic inference is more robust to overparameterization than underparameterization (Huelsenbeck and Rannala, 2004). In addition, the resulting topology was consistent with, though not identical to, the topology obtained by a Bayesian reversible-jump mixture model analysis of the same data set using BayesPhylogenies (Pagel and Meade, 2004), which employed two GTR + G models and no partitioning.

Experimental animals

We collected colonies of eight species of *Odontomachus* representing a range of body sizes and ecologies (Table 3), all of which were also included in the phylogenetic analysis. Colonies were maintained in the lab and fed a diet of mealworms, waxworms or crickets, three times per week. All data were collected as described below with the exception of *O. bauri* data, which were adopted from Patek et al. (Patek et al., 2006) without reanalysis and included with the other seven for comparison.

High-speed video and analysis

The protocol for filming of trap-jaw strikes was modified from Patek et al. (Patek et al., 2006), using a high-speed camera attached to a microscope (70 000–100 000 frames s^{-1}, 2–11 μs shutter speed; Ultima APX Photron, San Diego, CA, USA; Leica MZ 12.5 stereomicroscope). Ants were fixed using a drop of paraffin wax (applied to the top of the head) to the end of a rod that could be

rotated to keep the jaws perpendicular to the camera's axis. Animals were hung by this translating rod in an empty beaker and stimulated to strike by touching their 'trigger hairs' with a thin metal probe of known diameter (0.24 mm).

The kinematic data were used to calculate speed, acceleration and the lag time (if any) between the first jaw to close and the second. Custom software developed by the authors (available as Supplemental Items S1, S2 and S3 at http://www.life.uiuc.edu/suarez/datasets.html) in MATLAB (v. R2007a, Mathworks, Natick, MA, USA) was used to track the mandible movements and calculate their angular and tangential speeds and accelerations. An optimization technique was used whereby the root mean square (RMS) error was minimized with reference to the coordinates of the center of rotation and the size of each mandible. The mathematical challenge was to fit a circle to a sequence of traced points; the circle would be the mandible tip trajectory, and its center would be the center of rotation of the movement.

The code was composed of two parts: the first traced the paths of the jaws, and the second calculated speed and acceleration. Information from jaw-snap films was input into the tracing module, including resolution (in dpi), size (width and height in pixels), frame rate (frames s^{-1}) and the magnification factor of the microscope. Then, each frame in the sequence was displayed as a MATLAB figure and the position of the mandible tips was recorded in each frame. Also, the approximate position of the mandible base was recorded for the first and last frames. These data were then stored as two matrices of coordinates, one containing the mandible tip coordinates for each frame and the other containing the mandible base location; the latter were x and y coordinates averaged from the two sets. The data were then saved and loaded into the calculations program.

The calculations program first built a grid of possible centers of rotation about the averaged mandible base location. In addition, a column matrix was constructed for each mandible that contained the possible values of each radius for the traced circles. Using nested loops, iterations were performed on the values of the centers of rotation and radii for each mandible and the RMS error was calculated using the formula:

$$E(x_c, y_c, r) = \sqrt{\frac{1}{T}\sum_{t=0}^{S}\left\{\left[(x_i(t) - x_c)^2 + (y_i(t) - y_c)^2\right]^{0.5} - r\right\}^2}, \quad (1)$$

where T is the number of free parameters, x_c and y_c are the coordinates of the center of rotation, $x_i(t)$ and $y_i(t)$ are the coordinates of the traced points at frame (t), S is total number of frames tracked, and r is the radius of the best fitting circle (Kreyszig, 1999). Once the centers of rotation and radii were found for each mandible, the slopes of each were calculated throughout the sequence. From these slopes, the angles were extracted. Angular velocities were then calculated by multiplying the difference between slopes in radians with the number of frames per second. The same procedure was applied to the difference of angular velocities to obtain the angular accelerations. By using the dpi and magnification data, the radii were expressed in units of meters, such that, when multiplied by the angular velocities and accelerations, they would yield their linear, tangential counterparts. Velocity and acceleration profiles were plotted for each strike, as shown in Supplemental Item 1. The Matlab-compatible scripts are downloadable from Supplemental Items 2 and 3, and available from the authors upon request.

With accelerations derived from kinematic data (see above) and the mandible masses (see below) we calculated peak instantaneous force using the convention of Patek et al. (Patek et al., 2006). The moment of inertia for a thin rod of length R and mass M rotating around a fixed point (I=1/3MR^2) was used to calculate the force (defined as the perpendicular strike force of the tip of the mandible at α–max) as:

$$F_{max} = 1/3Mr\alpha\,, \quad (2)$$

where M is the jaw mass, R is the distance from the center of rotation to the jaw terminus, and α is the maximum angular acceleration (in radians s^{-2}).

Measurement error for digitization of strikes was estimating by re-tracking and recalculating a representative two-jaw strike from each of the frame rates used (70 000 frames s^{-1}, 90 000 frames s^{-1}, and 100 000 frames s^{-1}) five times, yielding a total of 12 single-jaw strikes for each re-tracked video segment. Percentage difference from the mean was then averaged across all 12 strikes at each frame rate.

Filtering data

Differentiation of point-tracking data to produce velocity and acceleration values has been considered problematic, particularly for acceleration data, as it requires second order differentiation and is likely to amplify tracking error (Walker, 1998). Subsequent 'choosing' of points of greatest acceleration, as we have done here, might be expected to systematically overestimate mean maximum acceleration values. We evaluated four combinations of methods for alternative calculation of maximum velocity and maximum acceleration of a subset of the data to determine whether our results could be improved by filtering. Both cubic and quintic splines were fitted to the data, and tracking sequences were differentiated using both two-point (the control, or baseline differentiation method) and three-point differentiation methods, yielding six means (linear, cubic and quintic spline fits, each with two differentiation methods). We chose to use unfiltered, two-point differentiated data, as the spline-fit data tended to slightly overestimate maxima, which did not solve our overestimation problem, and the three-point differentiations resulted in unrealistically low estimates (as much as 31% less) for acceleration, whether or not a spline curve was fitted to the data points. Plots comparing effects of the filtering techniques explored, can be seen in Supplemental Item 4.

Ant measurements, phylogenetic comparative methods, and scaling equations

We filmed four to six workers from each species and up to six strikes per worker. Total strikes recorded and analyzed per species ranged from 13 (*O. chelifer*) to 25 (*O. cephalotes*). Following jaw-snap recordings, individual worker ants were killed by freezing and stored in a –20°C freezer. To minimize changes in mass caused by drying, ants were stored in air-tight vials and all mass measurements were made within 10 days of freezing. We measured the following for each ant: whole-body mass, head length (clypeus to apex), and head width [including the eyes; after Hölldobler and Wilson (Hölldobler and Wilson, 1990)]. We then dissected out the mandibles of each ant and measured them individually for mass and length. Linear measurements were made using a Semprex Micro-DRO digital stage micrometer (0.005 mm resolution; Semprex Corporation, San Diego, CA, USA) connected to a Leica MZ 12.5 stereomicroscope, and masses were measured using a UMX2 microbalance with 0.1 μg resolution (Mettler-Toledo, Columbus, OH, USA).

Size measurements were $\log_{10}$ transformed, and TFSI [test for serial independence, as specified by Abouheif (Abouheif, 1999)] analyses were performed using our phylogenetic hypothesis in the software PI v. 2.0 (Reeve and Abouheif, 2003) to determine

whether any of the following (log transformed) measurements showed significant phylogenetic signal: head width, jaw length, body mass and jaw mass. Similarly, values for speed, acceleration, raw and normalized force were subject to the TFSI test to determine whether further statistical tests would be influenced by statistical non-independence due to phylogeny; ANOVA and *post-hoc* testing were only performed on species means that did not show significant phylogenetic signal in the TFSI test.

For scaling relationships, head width was used as a proxy for body size, as it is a standard measurement in the ant literature, and is a better predictor of body mass across the subfamily Ponerinae (Kaspari and Weiser, 1999) than head length, which we verified for our test species with RMA regression using RMA for Java (Bohonak and Van der Linde, 2004; Sokal and Rohlf, 1981), as r^2 for RMA regression of body mass *vs* head width=0.99, whereas r^2 for body mass *vs* head length=0.98. Except where otherwise cited, statistics were performed using Statistica software (version 6.0, StatSoft Inc., Tulsa, OK, USA), and plots were produced using Excel 2003 (Microsoft Inc., Seattle, WA, USA).

Because species values are not statistically independent, we used the method of independent contrasts (Felsenstein, 1985) as implemented in the program PDAP in the Mesquite comparative analysis package (Midford et al., 2005; Maddison and Maddison, 2006) to develop the scaling equations for jaw length, jaw mass and body mass, and to produce the regression line for angular acceleration (alpha) and head width. Continuous data for head width, jaw length, jaw mass, body mass, were $\log_{10}$ transformed and input into PDAP along with the topology and branch length data. With this information, PDAP provides hypothetical values for ancestral nodes and normalizes them to produce contrast values. The procedure of Garland et al. (Garland et al., 1999) was implemented to produce scaling equations for size parameters and to plot angular acceleration against head width. Linear ordinary-least-squares regressions with the intercepts set to the origin were performed on the normalized contrast values to calculate the slopes for the scaling equations. Biologically meaningful intercepts for scaling equations were calculated by substituting the mean values from the root nodes (which serve as estimates of the ancestral conditions) for the independent and dependent variable from each equation, the IC-corrected slope, and solving for the intercept value. Contrast values and resulting slopes were checked using independent contrasts derived in the Macintosh program CAIC (Purvis and Rambaut, 1995).

Modeling force production using scaling equations

To predict values for maximum force perpendicular to the jaw surface across a range of ant sizes based solely on scaling relationships, we parameterized Eqn. 2 using the scaling equations for jaw length and jaw mass (Eqn. 3 and Eqn. 4, see Results section) and angular acceleration, as functions of head width (Eqn. 6). This curve was also parameterized with scaling equations produced by phylogenetically uncorrected OLS regression on the species means for comparison between force production scalings that account for phylogeny, and those that do not.

RESULTS

Phylogeny

The phylogenetic hypothesis with relative branch lengths developed for all exemplar species from combined data is shown in Fig. 1. *Odontomachus* is monophyletic in the combined tree, with *Anochetus*, another genus of trap-jaw ants, as the most probable sister group. Nuclear-only and mitochondrial-only trees (not shown) differed only in the rooting of the *Odontomachus* clade and in the relative position of a single taxon (*O. ruginodis*), but the single-gene trees were supported by posterior probabilities 26% lower than our preferred, combined-data tree. Branch lengths for internal nodes in the *Odontomachus* clade appear to be short relative to those for terminal taxa in this group, and both topology and branch-length information from the combined-data tree were included in the subsequent comparative analyses.

Jaw usage patterns and temporal offsets

Five types of strike were seen: one jaw only (left or right), and two-jaw strikes with the left jaw leading, right jaw leading, or simultaneous closure. Leading jaw was defined as the jaw that achieved maximum acceleration toward the midline first; closures

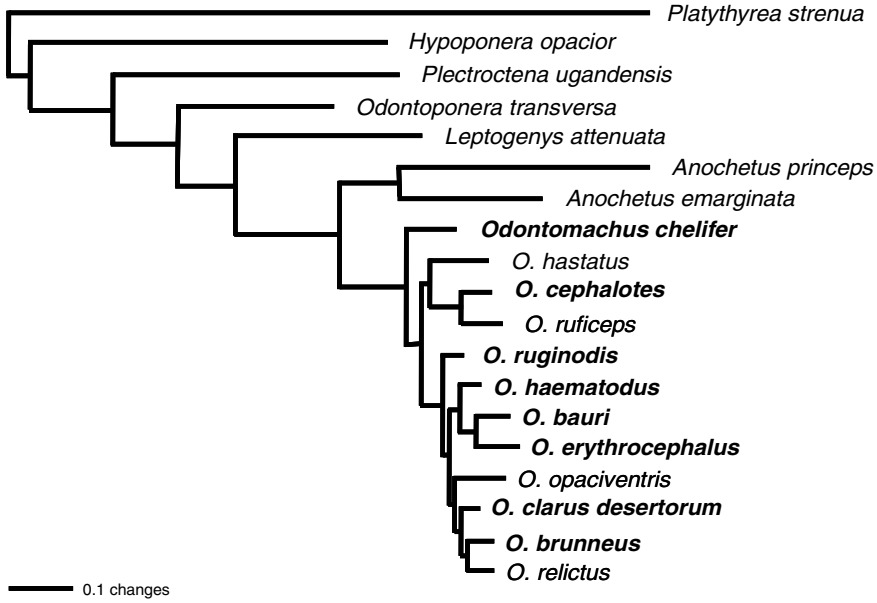

Fig. 1. Majority-rule combined-data Bayesian tree for taxa of interest and outgroups, with branch lengths proportional to genetic change. Names of species providing jaw-strike data are in bold.

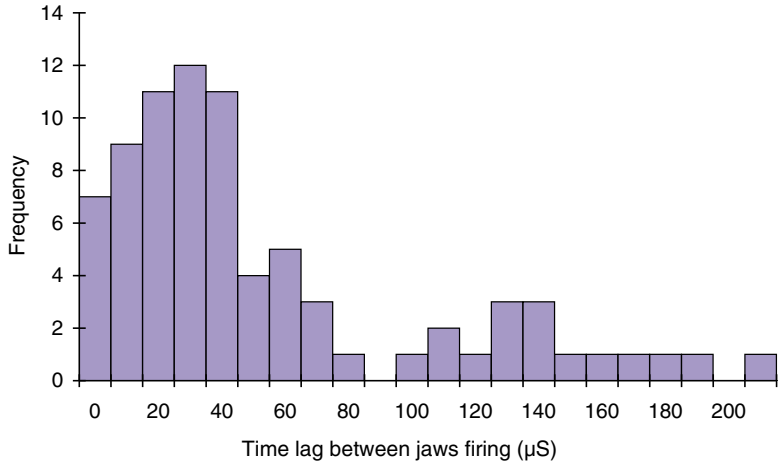

Fig. 2. Histogram of lag time between jaw firing in two-jaw strikes from all species (N=79 strikes), mode=30–40 μs, mean=54 μs. First bin represents simultaneous closure.

were considered simultaneous when the two maxima occurred in the same video frame. No significant pattern was seen within or between species in terms of a preference for a leading jaw in two-jaw strikes (34 were left-right, 38 were right-left; χ^2=0.22, P=0.64), whereas simultaneous closure occurred in seven of 79 two-jaw strikes. Single-jaw strikes appeared to favor the left side (38 left-only *vs* 18 right-only strikes, χ^2=7.14, P=0.007). All species examined included individuals that made both leading-right and leading-left strikes, and despite low strike numbers per individual, 11 of 25 individuals exhibited both types of strike, and the remaining 14 were evenly divided between 'left-dominant' and 'right-dominant' individuals.

Most strikes were two-jaw closures with one jaw beginning to close one or more frames after the first. The majority of two-jaw strikes (72 of 79 total strikes) included temporal offset, but due to extremely rapid acceleration of the second jaw, the second jaw often 'caught up' with the first, and the two jaws scissored past each other at or very near the midline of the ant's head. However, the jaws closed simultaneously in the remaining seven strikes, or so close to simultaneous that the tiny offset could not be resolved. Distribution in lag time between maximum jaw accelerations for all strikes can be seen in Fig. 2, with a mode of 30–40 μs. Distribution is unimodal with a long right-hand tail representing strikes with long between-jaw lags, where one jaw closes completely before the other begins to close.

Body size isometry

Across all species, the log–log regression slopes for independent contrast values for jaw length, jaw mass and body mass against head width (Fig. 3) did not allow rejection of the null hypothesis of isometry. Jaw length (P=0.0053, mean slope=1.12, 95% confidence interval for slope=0.61–1.63, r^2=0.75) scaled to the first power with body lengths, whereas the slope of ~3 for jaw mass (P=0.0018 man slope=3.26, 95% CI=2.07–4.45, r^2=0.82) and body mass (P<0.001, mean slope=2.94, 95% CI=2.03–3.85, r^2=0.87) indicated isometry between total body mass and head width (Fig. 2), as mass scales to the third power of linear size. The r^2 values were lower for jaw length than for length–mass plots (0.75 *vs* 0.82 and 0.87 for jaw mass and body mass, respectively), indicating that across species, jaw length may be more variable than body mass and jaw mass as a function of head width.

Scaling equations, expressed as functions of head width (h), across independent contrasts are as follows, with Eqns 3a, 4a and 5a calculated using independent contrast regressions, and Eqns 3b, 4b and 5b uncorrected:

$$R = 0.66h^{1.12}, \quad (3a)$$

$$R = 0.55h^{1.38}, \quad (3b)$$

$$M = 0.013h^{3.26}, \quad (4a)$$

$$M = 0.0084h^{3.73}, \quad (4b)$$

$$B = 1.45h^{2.94}, \quad (5a)$$

$$B = 1.26h^{3.16}, \quad (5b)$$

where R is jaw length, M is jaw mass and B is body mass.

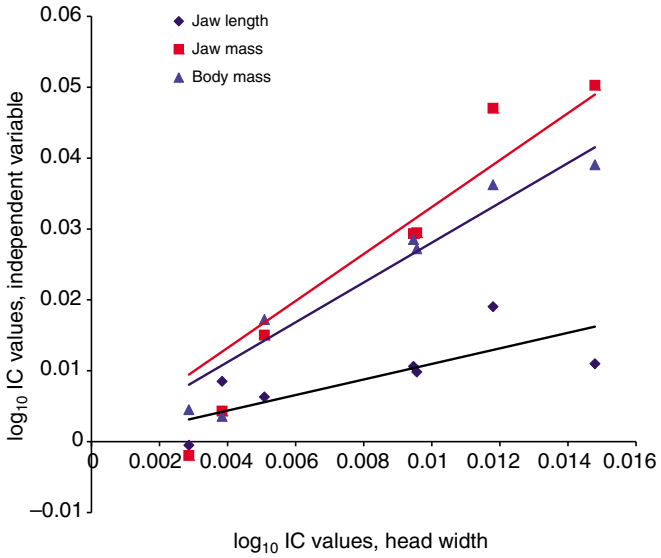

Fig. 3. Isometric scaling of independent contrast values for *Odontomachus* species. OLS regressions of normalized independent contrast values (IC) for body mass, jaw length and jaw mass against head width, with intercept set to the origin. All have slopes that do not depart significantly from null hypothesis of isometry for linear scaling (slope=1) or for mass scaling (slope=3), as follows: jaw length: P=0.0053, slope=1.12, 95% confidence interval for slope=0.61–1.63, r^2=0.75; jaw mass: P=0.0018 slope=3.26, 95% CI=2.07–4.45, r^2=0.82; body mass: P<0.001, slope=2.94, 95% CI=2.03–3.85, r^2=0.87.

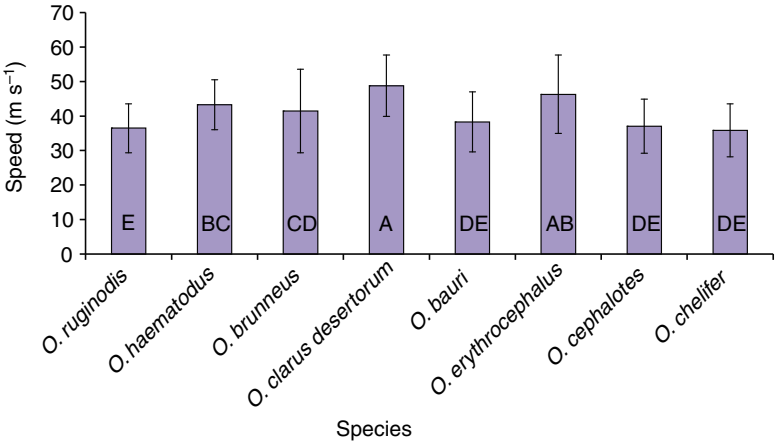

Fig. 4. Mean maximum radial speeds for all jaws of eight species of *Odontomachus*. One-way ANOVA significant (P<0.001). Species arranged from left to right by mean mass (lowest to highest). Species with the same letters (A–E) are statistically indistinguishable from each other at the P<0.05 level in *post-hoc* pairwise tests. Maximum jaw speeds of *O. clarus desertorum* and *O. erythrocephalus* (group A) are significantly higher than previous highest reported value for self-propelled prey strike in animals [*O. bauri* (Patek et al., 2006)].

Speed and acceleration

Mean maximum radial jaw speeds differed significantly among species (Fig. 4), ranging from 35.9±7.7 m s^{-1} in *O. chelifer* to 48.8±8.9 m s^{-1} in *O. clarus desertorum*, bracketing previously reported values for *O. bauri*. The three fastest-striking species (*O. haematodus*, *O. clarus desertorum* and *O. erythrocephalus*) differed significantly from the three slowest (*O. ruginodis*, *O. cephalotes* and *O. chelifer*), whereas *O. brunneus* did not differ significantly from either of these groups. Mean maximum jaw speed did not correlate significantly with head width or body mass (P>0.05), and phylogenetic signal was not significant for jaw speed using the TFSI test (P=0.21). Measurement error due to digitizing for speeds and accelerations averaged ±6% and ±11%, respectively.

Mean maximum angular accelerations varied from a value of 1.31×10^{9} radians s^{-2} in the smallest species (*O. ruginodis*) to 3.87×10^{8} radians s^{-2} in the largest (*O. chelifer*; Fig. 5A). With the TFSI test indicating that angular acceleration values showed significant phylogenetic non-independence (P=0.02), independent

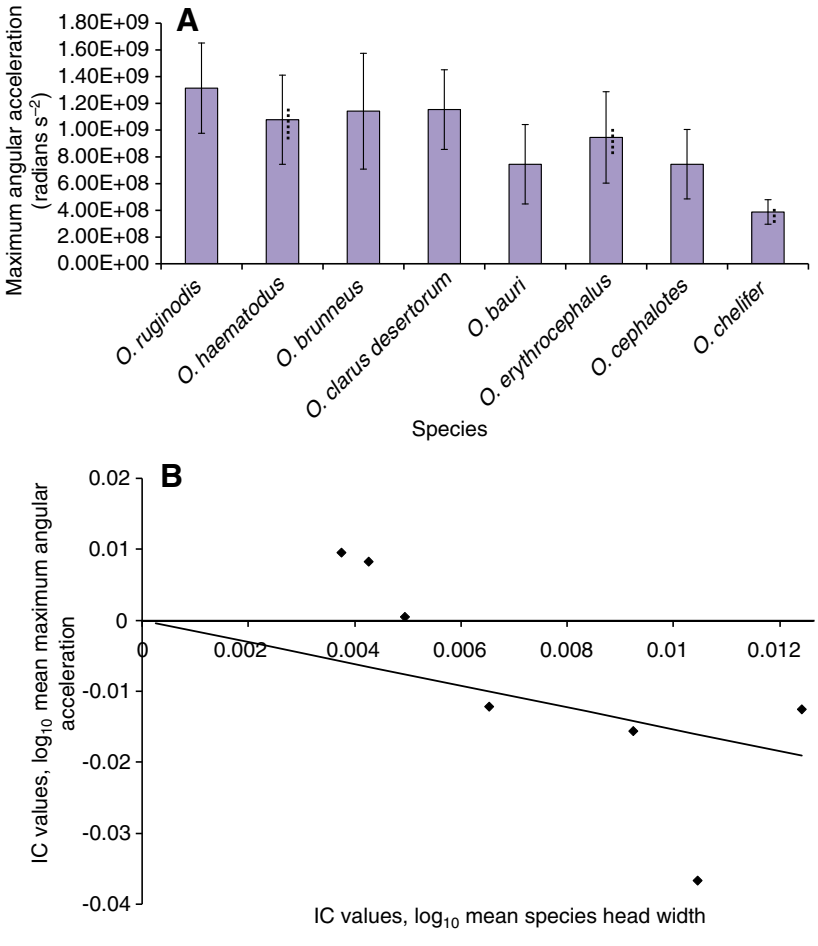

Fig. 5. (A) Mean (± s.d.) maximum angular acceleration (α) by species, in radians s^{-2}. Species arranged from lowest mean mass to largest, left to right. Secondary error bars (dotted lines) represent digitization error for groups in which this was estimated. (B) Scatterplot and regression of independent contrast (IC) values for $\log_{10}$-transformed jaw accelerations *vs* $\log_{10}$ head width (P=0.04, slope=–1.54, 95% CI=–2.72 to –0.354, r^2=0.52).

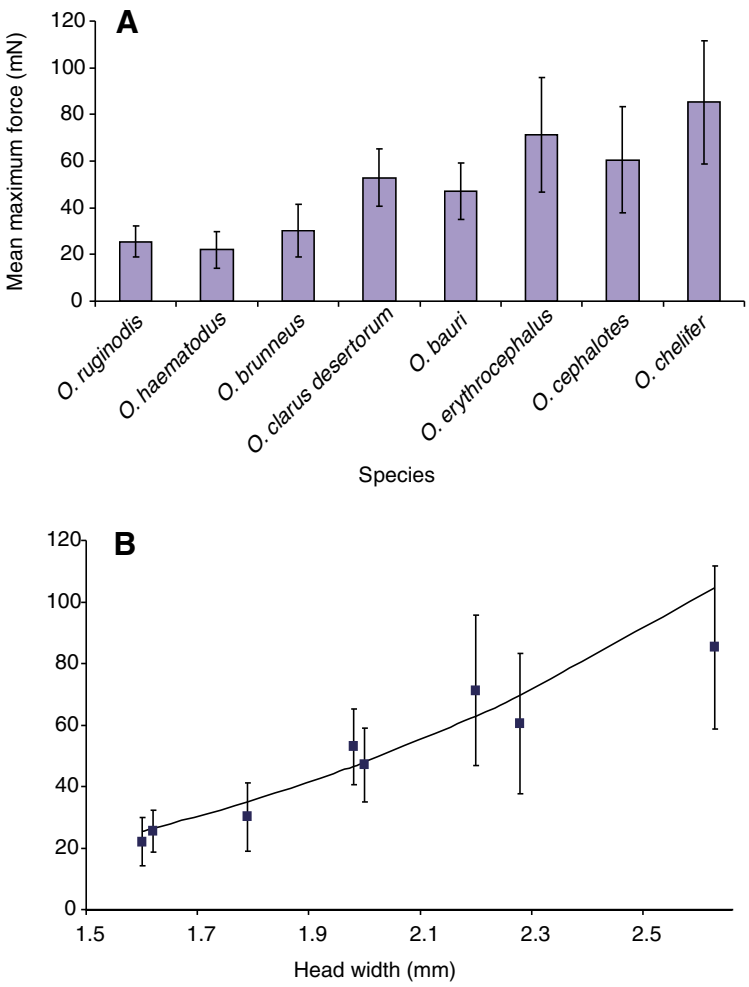

Fig. 6. (A) Mean maximum single-jaw forces (± s.d.), by species. Species arranged from lowest mean mass to largest, left to right Modeling force as a product of jaw length, jaw mass and maximum acceleration (see Eqn. 2) reveals significant differences in force production (one-way ANOVA, $P<0.001$). (B) Comparison of species means (squares) to model predictions from phylogenetic comparative model (line), with quantitative *x*-axis.

contrast values were calculated prior to further analysis. Regression of independent contrasts (IC values) of angular acceleration on head width ICs (Fig. 5B) yielded the following equation:

$$\alpha = 2.34 \times 10^{9} h^{-1.54}, \quad (6a)$$

(95% confidence interval for the scaling coefficient of –3.03 to –0.05) and the phylogenetically uncorrected species values yielded the following equation:

$$\alpha = 3.49 \times 10^{9} h^{-2.01}, \quad (6b)$$

(95% confidence interval of slope –3.44 to –0.58), where α is the angular acceleration in radians and h is the head width. Neither slope differs significantly from the null expectation of –2 that would be assumed if muscle cross sectional area scales isometrically.

Re-running the TSFI analysis following calculation of independent contrast results showed that phylogenetic signal was no longer significant when independent contrast values for acceleration were used (P=0.27).

Based on species means for maximum acceleration, jaw length and jaw mass, mean maximum single-jaw forces (Fig. 6A) ranged from 22±8 mN in *O. haematodus* to 85±26 mN in *O. chelifer*.

Predicting jaw performance based on size parameters

Predicting force production based on a single scaling parameter (head width) yielded a curve showing maximum single-jaw force production increasing a range of head widths. This was done by parameterizing Eqn. 2 by substituting Eqns 3a, 4a and 6a for M, R and α. Plotting model predictions for a range of head widths yielded the curve shown in Fig. 6B, with maximum jaw force continually increasing as a function of head width.

General predictions from modeling force production based on scaling equations (both phylogenetically corrected and uncorrected) were then compared to the forces estimated from the original species data (Fig. 7). Comparing species' measurement-based maximum force values with general size-based model predictions (as in Fig. 6B) showed a mean absolute difference of 12% when phylogeny was accounted for, and 11% when compared to the phylogenetically uncorrected model (Fig. 7). Size-based force predictions from phylogenetically corrected scalings differed from those made with uncorrected (or 'star phylogeny') scalings by an average of 3%.

DISCUSSION

The kinematic data presented here show a large range of jaw force-generation abilities in the genus *Odontomachus*: a nearly fourfold difference between the largest and smallest species, scaling with a related range of sizes but varying considerably (±12%) from strictly size-based expectations. In the context of the phylogeny, this variation gives us clues to which features may be most evolutionarily labile, giving rise to relatively high- and low-force producing species. Comparing phylogenetically corrected and star-phylogeny models suggests that differences in performance relative to the model may be due to relatively recent selection pressures.

Jaw-lag and jump performance

As in previous work on *O. bauri* (Gronenberg and Tautz, 1994; Patek et al., 2006), both mandibles rarely snapped shut synchronously. The lag between jaws followed the same general pattern previously demonstrated by Patek et al. (Patek et al., 2006), where lag time between individual pairs averaged ~40 μs; however, the synchronous closing in a small number of snaps (seven total strikes, in three species – *O. haematodus*, *O. clarus desertorum* and *O. cephalotes*) suggests the time-lag does not represent a minimum time for neural conduction from one mandible to the other. It is possible that the 'no lag' strikes are triggered differently from the strikes exhibiting the lag, perhaps by having both jaws stimulated simultaneously, assuming that most strikes result from a stimulation of the trigger-hairs on one side of the cocked mandibles and require conduction to the other jaw for firing of both jaws.

Alternately, there may be an adaptive explanation for a lag between mandibles if temporally off-set strikes either help prevent damage to the jaws if the target is missed or create greater force at impact with the second mandible as the target gets displaced towards the midline by the first. Jaw lag might also be expected to contribute to the jump trajectories of the ants, possibly introducing a rotation

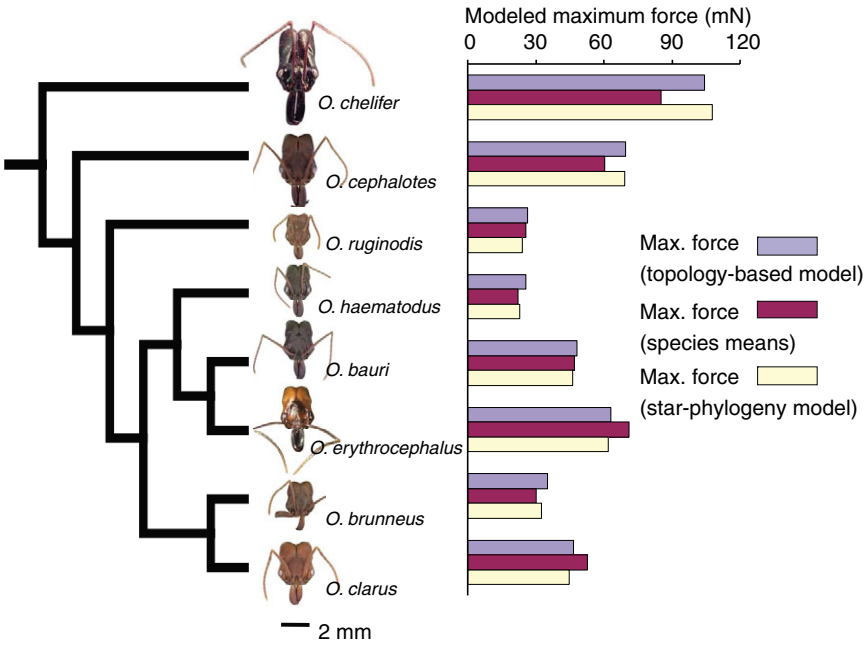

Fig. 7. Phylogeny, head size and force production in *Odontomachus*. Head sizes are species means, scaled to 2 mm bar. Bar graph shows force production predicted by independent-contrast model (blue bars), species mean data (maroon bars), and star-phylogeny model (beige bars) for each species studied. Forces calculated from actual species means differed from head width-based predictions from phylogenetically corrected models by an absolute mean value of 12%, and from the uncorrected models by 11%. Predictions derived from uncorrected (star-phylogeny) and phylogeny-corrected models differed by an average of 3%.

about the ants' head-to-vent axis, or tending to throw the animal sideways rather than vertically. However, without a model that translates jaw speed and acceleration into jump performance, and video data from jump sequences that can resolve distances, angles and speeds of individual jaws as they contact substrates during the acceleration phase of jumps, this hypothesis cannot be tested. The lack of such a model also limits our ability to make predictions about jump performance with the current dataset, as existing models for jumping are based on acceleration during extension of jointed legs (e.g. Alexander, 1995) rather than rapid rotation of opposing fixed-end jaws against a substrate.

Scaling and force-production in trap-jaw ants

Morphological variation across the eight species of *Odontomachus* examined here showed the simplest pattern of differentiation (Wheeler, 1991; Wilson, 1953), where worker variation follows a continuous, linear isometric or allometric curve. Without a larger sampling regime, it is impossible to reject among-species variation along slopes that conform to the simplest submodel of continuous linear variation, that of isometry. This contrasts with the allometric, clearly differentiated morphological castes (Wilson, 1976), found in some species of polymorphic ants.

Under any scaling model, maximum force, as a product of jaw mass, jaw length and angular acceleration, would be tightly linked to mandible mass and length. As seen here, in even the slowest-accelerating *Odontomachus* examined (*O. chelifer*), large values for mass and length compensated for reduced acceleration, resulting in a fourfold greater force generation than seen in the smallest species (*O. ruginodis*), despite the latter having the highest mean maximum angular acceleration of the species studied. Species mean values generally track model predictions well, with variation from model predictions falling within standard deviations for all eight species. Despite the positive relationship between maximum force and size, there appears to be no clustering of species at the high end of the range of sizes seen, nor is there any obvious trend toward larger size in more derived species in the phylogeny.

It is worth noting that when *not* performing full lock-and-release strikes, *Odontomachus* ants have been shown to have some of the slowest jaw movements of any ants, as their adductor muscles, though quite large, are composed almost entirely of long-sarcomere, slow-contracting fibers (Gronenberg et al., 1997). Most ants have a mixture of long- and short-sarcomere fibers in their jaw adductors, and their jaw movements may be five to ten times faster than non-power-amplified *Odontomachus* jaw closures (Gronenberg et al., 1997; Paul and Gronenberg, 2002). The low speeds of normal jaw movements do not appear to be a problem for these ants, as the workers are generally monomorphic and can perform all nest tasks (carrying food, moving larvae and eggs, moving nesting materials) using their oversized, slow-contracting jaws.

Of the species studied, *O. chelifer* is the clear champion in terms of force production (Fig. 6A). Laboratory observations (A.V.S. and J.C.S., unpublished data) show that these robust ants do indeed deliver devastating strikes, such that they seldom, if ever, use their stings in attacks on prey animals – a single strike is usually enough to disable the prey item. This is in contrast to smaller species, which generally strike and subsequently sting to disable prey.

With continuous, log-linear size variation and multiple species with workers considerably smaller than the largest *Odontomachus* species, it appears that optimal size for a particular species is not dependent on maximum force production. More likely, in such an isometric context, maximum size is balanced against the developmental and physiological costs of growing and carrying (and loading) oversized adductor muscles and jaws. Alternative hypotheses need to be examined including those relating to 'optimal speeds' for capturing elusive prey such as springtails (Brown and Wilson, 1959), or 'ecological release' relative to jaw performance – wherein there is no natural enemy or prey item requiring such extreme speed or force production, so that individual size is determined by other selective pressures, such as food availability or optimal size relative to available nesting sites. In other ant lineages where trap-jaw morphologies have evolved independently, including taxa in the Myrmicinae (Gronenberg, 1996b) and Formicinae (Moffett, 1985) subfamilies, we might expect to see similar species-scaled differences in performance, although isometric scaling cannot be assumed for these.

Although the workers of most *Odontomachus* species show little variation in size within a single colony, some species do have

workers within a colony that exhibit a range of sizes (e.g. *O. cephalotes*, a Northern Australian species). Detailed study of species with broad intra-specific distribution of worker sizes, including characterization of behavior of individuals by size and age, will help determine how trap-jaw phenotypes are tuned by the social environment, development and evolutionary history. More generally, greater within-species sampling and narrowly focused study of species that may deviate from the log-linear relations presented here will be valuable in understanding the selective pressures contributing to diversity (Biewener, 2003) in trap-jaw ants.

The predictions of this paper should also be tested *via* direct measurements of force production across these (and other) *Odontomachus* species. The behavioral ecology, including prey and natural enemy types, and relative frequency and ecological correlates of jaw usage (jumps *vs* strikes) remains largely unknown, and may help explain the preponderance of relatively small species.

Phylogenetic comparative methods

The *Odontomachus* phylogeny developed here, with its relatively short internal branches, suggests the possibility that this genus diversified quickly, with fewer subsequent speciation events following an original radiation, or an increase in extinction rate leaving relatively long terminal branches. Alternatively, our sampling regime may have been broad enough and evenly distributed enough to create relatively long branches as an artifact. In either case, it approximates the 'star phylogeny' assumed in use of non-phylogenetically corrected species data, and is less likely to be confounded by an uneven distribution of recently and less-recently diverged species (Garland et al., 1999; Price, 1997). Despite this, the results of the TFSI tests demonstrated significant phylogenetic signal in key parameters expected to influence force production, particularly jaw acceleration, arguing for incorporation of statistical methods correcting for phylogeny.

We found only small differences between jaw-strike forces predicted by the phylogenetically corrected and uncorrected models for force production. However, there is still significant value added when the data are viewed in the context of the phylogeny, both from first principles and in terms of the quality of results for purposes of additional hypothesis generation and testing. First, without a phylogeny, there is no *a priori* way to know what the effect of accounting for branching patterns and branch lengths would be, and the assumption that it will not influence the outcome has been shown to be incorrect in numerous studies (e.g. Nunn and Barton, 2000; Zani, 2000; Smith and Cheverud, 2004). Second, given that the data appear to contain phylogenetic signal according to the TFSI tests, but that accounting for that signal does not necessarily improve predictions of force-generation performance for the actual terminal taxa, we can make inferences about evolution of the trap-jaw system that would otherwise be difficult to support. In the present study, the situation where phylogenetic signal may exist but does not account for the differences in performance between taxa may be a case like that presented by Price (Price, 1997) where a variable character has been under recent selection in the individual species' environments, and the contrast data, representing relatively deep divergences, can be overwhelmed by recent adjustments in the character – in this case, body size, with performance scaling in simple isometry with changes in size.

The authors thank Brian Fisher of the California Academy of Sciences, Chris Smith of University of Illinois and Mark Deyrup of the Archbold Field Station for assistance in collecting and maintaining ant colonies, and Joe Baio and Tawny Mata for assistance with filming strikes and data processing. We also thank the following individuals for loan of specimens for phylogenetic analyses: Lloyd Davis, David Donoso, Kim Franklin, Jurgen Liebig, David Maddison, John Mangold, Wendy Moore, Maruyama Munetoshi, Chris Smith and Alex Wild. For permission to collect and import ants, we thank the Ministry of Environment and Energy (Permit 122-2004-OFAU) of Costa Rica, the Ministerio de Salud y Ambiente (Permit 20202/05) of Argentina, the Administracion de Parques Nacionales (Permit 002870-2) of Argentina, James Cook University, Australia for the loan of *O. cephalotes* specimens and the United States Department of Agriculture (APHIS import permit 69963). This work was supported by a seed grant from the Beckman Institute for Advanced Science and Technology.

REFERENCES

Abouheif, E. (1999). A method to test the assumption of phylogenetic independence in comparative data. *Evol. Ecol. Res.* **1**, 895-909.
Abouheif, E. and Wray, G. A. (2002). Evolution of the gene network underlying wing polyphenism in ants. *Science* **297**, 249-252.
Alexander, R. M. (1995). Leg design and jumping technique for humans, other vertebrates, and insects. *Philos. Trans. R. Soc. Lond. B Biol. Sci.* **347**, 235-248.
Belshaw, R. and Quicke, D. L. J. (1997). A molecular phylogeny of the Aphidiinae (Hymenoptera: Braconidae). *Mol. Phylogenet. Evol.* **7**, 281-293.
Bennet-Clark, H. C. and Lucey, E. C. A. (1967). The jump of the flea: a study of the energetics and a model of the mechanism. *J. Exp. Biol.* **47**, 59-76.
Biewener, A. A. (2003). Physical and biological properties and principles related to animal movement. In *Animal Locomotion*, pp. 1-14. Oxford: Oxford University Press.
Bohonak, A. J. and Van der Linde, K. (2004). RMA: software for reduced major axis regression, Java version. http://www.kimvdlinde.com/professional/rma.html.
Brown, W. L. and Wilson, E. O. (1959). The evolution of the dacetine ants. *Q. Rev. Biol.* **34**, 278-294.
Carlin, N. F. and Gladstein, D. S. (1989). The 'bouncer' defense of *Odontomachus ruginodis* and other odontomachine ants (Hymenoptera: Formicidae). *Psyche* **96**, 1-19.
Deyrup, M. and Cover, S. (2004). A new species of *Odontomachus* ant (Hymenoptera: Formicidae) from inland ridges of Florida, with a key to *Odontomachus* of the United States. *Fla. Entomol.* **87**, 136-144.
Felsenstein, J. (1985). Phylogenies and the comparative method. *Am. Nat.* **125**, 1-15.
Garland, T., Midford, P. E. and Ives, A. R. (1999). An introduction to phylogenetically based statistical methods, with a new method for confidence intervals on ancestral values. *Am. Zool.* **39**, 374-388.
Gronenberg, W. (1995a). The fast mandible strike in the trap-jaw ant *Odontomachus*. 1. Temporal properties and morphological characteristics. *J. Comp. Physiol. A* **176**, 391-398.
Gronenberg, W. (1995b). The fast mandible strike in the trap-jaw ant *Odontomachus*. 2. Motor control. *J. Comp. Physiol. A* **176**, 399-408.
Gronenberg, W. (1996a). Fast actions in small animals: springs and click mechanisms. *J. Comp. Physiol. A* **178**, 727-734.
Gronenberg, W. (1996b). The trap-jaw mechanism in the dacetine ants *Daceton armigerum* and *Strumigenys sp. J. Exp. Biol.* **199**, 2021-2033.
Gronenberg, W. and Tautz, J. (1994). The sensory basis for the trap-jaw mechanism in the ant *Odontomachus bauri*. *J. Comp. Physiol. A* **174**, 49-60.
Gronenberg, W., Paul, J., Just, S. and Hölldobler, B. (1997). Mandible muscle fibers in ants: fast or powerful? *Cell Tissue Res.* **289**, 347-361.
Hölldobler, B. and Wilson, E. O. (1990). *The Ants*. Cambridge, MA, USA: Harvard University Press.
Huelsenbeck, J. P. and Rannala, B. (2004). Frequentist properties of Bayesian posterior probabilities of phylogenetic trees under simple and complex substitution models. *Syst. Biol.* **53**, 904-913.
Huelsenbeck, J. P. and Ronquist, F. (2001). MRBAYES: Bayesian inference of phylogenetic trees. *Bioinformatics* **17**, 754-755.
Just, S. and Gronenberg, W. (1999). The control of mandible movements in the ant *Odontomachus*. *J. Insect Physiol.* **45**, 231-240.
Kaspari, M. and Weiser, M. D. (1999). The size-grain hypothesis and interspecific scaling in ants. *Funct. Ecol.* **13**, 530-538.
Kreyszig, E. (1999). Method of least squares. In *Advanced Engineering Mathematics*, pp. 914-916. New York: John Wiley and Sons.
Maddison, W. P. and Maddison, D. R. (2005). *MacClade: Analysis of Phylogenetic and Character Evolution*. Sunderland, MA: Sinauer and Associates.
Maddison, W. P. and Maddison, D. R. (2006). Mesquite: a modular system for evolutionary analysis. Version 1.1. http://mesquiteproject.org.
Midford, P. E., Garland, T., Jr and Maddison, W. P. (2005). PDAP Package of Mesquite. Version 1.07. http://www.mesquiteproject.org/pdap_mesquite
Moffett, M. W. (1985). Trap-jaw predation and other observations on two species of *Myrmoteras* (Hymenoptera: Formicidae). *Social Insects* **33**, 85-99.
Nunn, C. L. and Barton, R. A. (2000). Allometric slopes and independent contrasts: a comparative test of Kleiber's Law in primate ranging patterns. *Am. Nat.* **156**, 519-533.
Pagel, M. D. and Meade, A. (2004). A mixture model for detecting pattern-heterogeneity in gene sequence or character-state data. *Syst. Biol.* **53**, 571-581.
Patek, S. N., Korff, W. L. and Caldwell, R. L. (2004). Deadly strike mechanism of a mantis shrimp. *Nature* **428**, 819-820.
Patek, S. N., Baio, J. E., Fisher, B. L. and Suarez, A. V. (2006). Multifunctionality and mechanical origins: ballistic jaw propulsion in trap-jaw ants. *Proc. Natl. Acad. Sci. USA* **103**, 12787-12792.
Paul, J. and Gronenberg, W. (2002). Motor control of the mandible closer muscle in ants. *J. Insect Physiol.* **48**, 255-267.
Price, T. (1997). Correlated evolution and independent contrasts. *Philos. Trans. R. Soc. Lond. B Biol. Sci.* **352**, 519-529.
Purvis, A. and Rambaut, A. (1995). Comparative-analysis by independent contrasts (CAIC) an Apple-Macintosh application for analyzing comparative data. *Comput. Appl. Biosci.* **11**, 247-251.

Rambaut, A. and Drummond, A. J. (2004). Tracer v1.3. http://beast.bio.ed.ac.uk/Tracer.
Reeve, J. and Abouheif, E. (2003). Phylogenetic Independence, Version 2.0. http://biology.mcgill.ca/faculty/abouheif/
Schmitz, J. and Moritz, R. F. A. (1994). Sequence analysis of the D1 and D2 regions of 28S rDNA in the hornet (*Vespa crabro*) (Hymenoptera, Vespinae). *Insect Mol. Biol.* **3**, 273-277.
Simon, C., Frati, F., Beckenbach, A., Crespi, B., Liu, H. and Flook, P. (1994). Evolution, weighting, and phylogenetic utility of mitochondrial gene sequences and a compilation of conserved polymerase chain reaction primers. *Ann. Entomol. Soc. Am.* **87**, 651-701.
Smith, R. J. and Cheverud, J. M. (2004). Scaling of sexual dimorphism in body mass: a phylogenetic analysis of Rensch's rule in primates. *Int. J. Primatol.* **23**, 1095-1135.
Sokal, R. R. and Rohlf, F. J. (1981). *Biometry*. New York: Freeman.
Walker, J. A. (1998). Estimating velocities and accelerations of animal locomotion: a simulation experiment comparing numerical differentiation algorithms. *J. Exp. Biol.* **201**, 981-995.
Ward, P. S. and Downie, D. A. (2005). The ant subfamily Pseudomyrmecinae (Hymenoptera: Formicidae): phylogeny and evolution of big-eyed arboreal ants. *Syst. Entomol.* **30**, 310-335.
Weibel, E. R. and Taylor, C. R. (1998). *Principles of Animal Design*. Cambridge: Press Syndicate of Cambridge University.
Wheeler, D. (1991). The developmental basis of worker caste polymorphism in ants. *Am. Nat.* **38**, 1218-1238.
Wheeler, W. M. (1922). Observations of *Gigantiops destructor* Fabricius and other leaping ants. *Biol. Bull.* **42**, 185-201.
Wild, A. and Maddison, D. R. (2008). Evaluating nuclear protein-coding genes for phylogenetic utility in beetles. *Mol. Phylogenet. Evol.* doi:10.1016/j.ympev.2008.05.023
Wilson, E. O. (1953). The origin and evolution of polymorphism in ants. *Q. J. Biol.* **28**, 136-156.
Wilson, E. O. (1976). Behavioral discretization and the number of castes in an ant species. *Behav. Ecol. Sociobiol.* **1**, 151-154.
Zani, P. A. (2000). The comparative evolution of lizard claw and toe morphology and clinging performance. *J. Evol. Biol.* **13**, 316-325.